Photon management modeling and beyond for photovoltaics

Peter Bermel *

Purdue University, Electrical & Computer Engineering, Birck Nanotechnology Center, 1205 West State Street, Room 2270, West Lafayette, IN 47907, USA

ARTICLE INFO

ABSTRACT

Improving the performance of photovoltaics is important for increased deployment in a broad range of applications. In this article, it is shown that combining detailed models for full-wave optics with one or more other physics models represents an emerging field of research. In particular, connections are made with geometric optics, electronic transport, and thermal transport. First, structures combining random texturing and periodic gratings offer the promise of higher light-trapping performance for a broad range of thin-film photovoltaic systems. Second, combining full-wave optics with electronic transport creates an opportunity to accurately model the limits of performance for devices approaching the Shockley–Queisser limit. Finally, combining optical with thermal modeling creates the potential for a physics-based understanding of intrinsic photovoltaic module failures, necessary to ensure a long life for photovoltaic cells.

1. Introduction

Every day, enough sunlight strikes the surface of the earth to supply the world's energy needs for the next 20 years [1,2]. However, the tremendous potential of this resource is tempered by the current expense of converting raw sunlight into electricity. In order to bridge this disconnect, the National Academy of Engineering has formulated the following grand engineering challenge: "make solar energy economical."

Solar photovoltaic conversion methods can be broadly divided into crystalline wafer-based and alternative approaches. Recent world records have been set for wafer-based cells with one to three distinct photovoltaic absorber materials: 28.3% for GaAs single junctions, 36.9% for GaInP/GaAs tandem cells, and 43.5% for triple-junctions of GaInP/GaAs/GaInNAs under 418 sun concentration [3]. Alternative photovoltaic technologies generally offer a substantial discount of 15–20% in cost relative to crystalline wafer-based cells, at the expense of lower maximum efficiencies [4–27]. One type of alternative PV technology is thin-film inorganic cells [4–10]. Examples include copper indium gallium selenide (CIGS) with record efficiencies of 20.4% [3,11–15], cadmium telluride (CdTe), with record efficiencies of 16.1% [3,16], and tandem silicon micromorph cells, with record efficiencies of 13.4% [3,17,18]. Other alternative PV technologies include organic PV cells, with record efficiencies of 10.7% [3,19–24], and dye-sensitized solar cells, with record efficiencies of 11.9% [3,25–27].

In principle, a range of these materials, having bandgaps well-matched to the solar spectrum and high electronic mobilities, are capable of approaching the Shockley–Queisser limit [28,29]. However, approaching this limit in general is a challenging problem, due to multiple charge carrier loss mechanisms beyond those assumed in the SQ limit, including but not limited to Shockley–Read–Hall, Auger and higher order carrier recombination processes in bulk, at grain boundaries, and surfaces, as well as Schottky barriers, and contact resistance [1,2,30–32]. Additional challenges associated with incoming sunlight include front-contact shadowing, reflection, and incomplete optical absorption, as well as parasitic loss mechanisms such as free carrier absorption and Ohmic absorption losses in metals [33–36].

Accurately predicting the performance of any solar cell under standard test conditions requires a combination of suitable models and experimental data for elementary material properties. Traditional modeling approaches have approximated elementary material properties from experimental observations; the electronic transport processes have been modeled in a semiclassical framework using the drift–diffusion model [37–40], and photon transport processes have been treated using an analytical expression such as Beer's law. However, more sophisticated full-wave optics models (using Maxwell's equations without approximations), such as finite-difference time domain simulations, have become increasingly prevalent [41–44].

In this paper, consideration is given to how one can combine these full-wave models of photon management with other physical effects which give rise to problems of great significance. Section 2 begins with a discussion of the mathematical models underlying the analysis in the remainder of this manuscript. Section 3 presents the first example of subrandom noise, which

---

* Tel.: +1 7654967879; fax: +1 7654944731.
E-mail address: pbermel@purdue.edu

combines full-wave optics with geometric optics effects. This is followed by a discussion of photon recycling in Section 4. In Section 5, the impact of photon management on intrinsic reliability is considered, as mediated through localized heating. Finally, this paper concludes by summarizing the state of the literature as well as future prospects.

2. Mathematical models

The overall power conversion efficiency of the PV diode is given by [1]

$$\eta = \frac{J_{sc}V_{oc} \times FF}{P_{sun}} \tag{1}$$

where V_{oc} is the open-circuit voltage, J_{sc} is the short-circuit current, FF is the fill-factor, and P_{sun} is the net power received from the Sun.

The open circuit voltage is given by [18]

$$qV_{oc} = E_g - nk_BT \ln\left(\frac{A}{J_{sc}}\right), \tag{2}$$

where E_g is the bandgap of the PV material, n is the ideality factor, q is the elementary charge, k_B is the Boltzmann constant, T is the temperature, and A is the recombination term, consisting of radiative recombination and Shockley–Read–Hall recombination mechanisms, given by [29]

$$A = \frac{q(\varepsilon+1)E_g^2 k_BT}{4\pi^2\hbar^3 c^2} + \frac{4qD}{L_DN_D}\left(\frac{k_BT\sqrt{m_e^*m_h^*}}{2\pi\hbar^2}\right)^3, \tag{3}$$

where ε is the dielectric permittivity, $\hbar$ is Planck's constant, c is the speed of light, D is the diffusion coefficient, L_D is the diffusion length, N_D is the defect density, and m_e^* and m_h^* are the effective masses for electrons and holes, respectively. In general, additional terms such as Auger recombination can be added in the presence of high injection currents. In any case, the dark current is then given by $J_s = Ae^{-E_g/nk_BT}$.

The fill factor FF can be estimated with the expression for FF_{sh}, which can be calculated in three steps [1]:

$$FF_o = \frac{z_{oc} - \ln(z_{oc}+0.72)}{z_{oc}+1} \tag{4a}$$

$$FF_s = FF_o[1-1.1r_s]+0.185r_s^2 \tag{4b}$$

$$FF_{sh} = FF_s\left[1-\left(\frac{V_{oc}+0.7}{V_{oc}}\right)\frac{FF_s}{r_{SH}}\right] \tag{4c}$$

where $z_{oc} = qV_{oc}/nk_BT$ is the reduced open-circuit voltage, $r_s = I_{sc}R_s/V_{oc}$ is the reduced series resistance, and $r_{sh} = I_{sc}R_{sh}/V_{oc}$ is the reduced shunt resistance.

The short circuit current J_{sc} is given by

$$J_{sc} = \frac{q}{hc}\int_0^\infty d\lambda \ EQE(\lambda)\frac{\lambda}{\lambda_g}\frac{dI}{d\lambda}, \tag{5}$$

where $dI/d\lambda$ is the wavelength-dependent AM1.5 solar spectrum, λ_g is the bandgap wavelength, and $EQE(\lambda)$ is the external quantum efficiency. The latter can be obtained using a drift–diffusion electronic transport model (ADEPT 2.0), which is freely available on nanoHUB.org [37].

Absorptivity is calculated using the finite-difference time domain method, as implemented in MEEP, and freely available on nanoHUB.org [41].

Modeling of thermal transport can be achieved on a standard finite-element mesh, employing the Galerkin method of converting the PDE for heat conduction into a sparse eigenvalue problem [42–44]. This allows us to implement both Maxwell's equations and the heat conduction equation in the same mathematical framework:

$$MH''+(K+\gamma^2M)H = 2\gamma H' \tag{6}$$

$$C\dot{T}+(K+G)T = \frac{\sigma}{\omega^2}(\nabla \times H)^2 + L \tag{7}$$

where H is the transverse magnetic field, T is the temperature field, M is the mass matrix, representing the (generally sparse) overlap between basis elements, K is the global matrix, capturing the wave physics of Maxwell's equation, γ is the average wavevector inside the structure, C is the heat capacity matrix, K is the heat conductivity matrix, G is the surface heat transfer matrix, σ is the electric conductivity, and L is the boundary condition (potentially a fixed temperature, convection, or thermal radiation). Implementations include the MATLAB toolbox known as FAESOR [42], as well as COMSOL [44].

3. Subrandom noise structures

Geometric light trapping enhancement is the traditional foundation for light trapping in photovoltaic structures. The general approach is to randomly scatter incoming light over a broad range of angles inside a high-index photovoltaic material, while placing a mirror on the bottom to redirect light back into the cell without impairing its ability to gather light. Combining these effects can yield a substantial $4n^2$ enhancement in the effective optical path length for bulk absorbers in the ideal case [45–47]. However, these techniques have been known for 129 years; after many generations of improvements, a performance plateau may have been reached for most bulk absorber designs.

However, for photovoltaic devices made from thin-films or incorporating other nanoscale features, the previous limits derived under the assumptions of classical optics no longer apply. Instead, wave optics dictates new limits on path length enhancement; it has been shown to be capable, in principle, of outperforming all geometrical optics approaches, for effective path length enhancements exceeding $4n^2$ [48–50]. This is particularly true over narrow bandwidths, because, in contrast to geometrical optics approaches that treat all wavelengths of light equally, wave optics approaches can be targeted to enhance absorption only in the range where it can be most beneficial [51–58]. However, it has been shown that there are also new limits to the bandwidth and absolute degree to which light trapping can be enhanced [50]. The major strategy for light trapping that has emerged recently is using periodic media such as gratings and photonic crystals, which strongly interact with light in key wavelengths of the solar spectrum. However, for PV cells made from broadband absorbers with limited demonstrated efficiencies and external quantum efficiencies, such as thin film silicon [17,18,51–55], organics [19–24,56–58], and CZTS [59–62], a single periodic structure may not yield the maximum possible enhancement at every wavelength of interest.

The obvious solution to the limits of periodic structures might at first appear to be to combine them all together. However, this approach encounters a major difficulty. If one chooses a tailored periodic structure for every wavelength one would like to trap, combine them together in Fourier-space, and then transform to real space, the end result is a spatially inhomogeneous system, as shown on the left-hand side of Fig. 1.

Thus, further major advances in photovoltaic performance are likely to arise from entirely new techniques for light trapping, which restore spatial homogeneity. At least two approaches warrant further consideration: direct homogenization, through Fourier randomization, and implicit homogenization, through quasicrystals. What they have in common is a set of Fourier components emphasized (technically, in the structure factor),
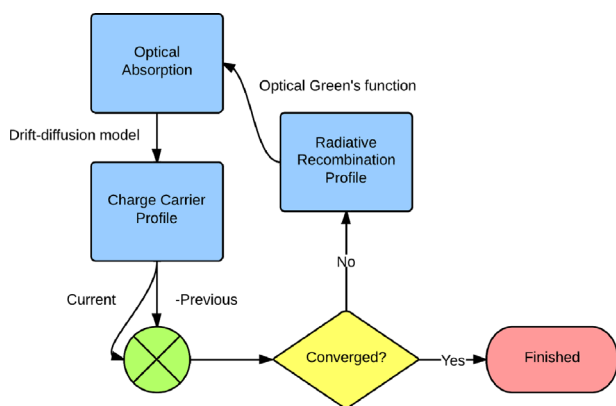
Fig. 1. Illustration of the premise of subrandom noise light trapping. Since the solar spectrum contains many wavelengths, it might naively make sense to combine gratings for each wavelength requiring light trapping. However, doing so directly yields a spatially inhomogeneous combined grating. On the other hand, if certain spatially periodic components (like gratings) are combined with a certain amount of noise, spatial homogeneity is restored, making it appropriate for uniform illumination from a wide range of wavelengths generally observed for photovoltaic cells.

Fig. 2. Conceptual approach to photon recycling calculation. The optical absorption associated with a given photovoltaic structure is fed into a drift–diffusion model. This produces a charge carrier distribution, and subsequently, a radiative recombination profile that feeds back into the optical absorption. This iterative feedback loop then converges to a stable charge carrier profile.

so as to induce diffraction of unconcentrated sunlight into oblique angles. The conceptual approach is shown in the right-hand side of Fig. 1. If certain spatially periodic components (like gratings) are combined with a certain amount of noise, spatial homogeneity is restored, making it appropriate for uniform illumination from a wide range of wavelengths generally observed for photovoltaic cells to enhance the effective path length of light by a factor of 30 in 2D, or a factor of 100 in 3D, substantially exceeding the performance over a broad bandwidth (e.g., for silicon thin-film tandem PV, from 650 to 900 nm) compared to any of the incumbent light trapping technologies mentioned above.

In the first case of Fourier randomization, it has been shown that enhancement in 2D substantially exceeds that of a flat structure by over 600%, as well as a uniform random structure, at the expense of angular insensitivity [63]. In the latter case of quasicrystals, it has been shown that enhancement exceeds that of a uniformly periodic structure [64]. However, it is clear that there is great promise for further work in this area, in terms of the classification, optimization, fabrication, and characterization of realistic 3D structures.

4. Photon recycling

Another example where traditional models cannot always accurately represent certain physical effects is the recapture (or recycling) of radiatively recombined photons. Radiative recombination is an inevitable part of solar cell operation at the maximum power point [30], which is incorporated into the Shockley–Queisser calculations [28,29]. There is generally a large difference between internal and external radiative recombination, caused by the large difference in the density of optical photon modes in III–V semiconductors compared to free space [65]. As a result of this effect, it is common that high-performance III–V solar cells, such as the 28.8% cells fabricated by Alta Devices [3,38,39], will re-absorb re-radiated photons many times before a terminal process (namely, external emission or non-radiative recombination) takes place.

The conceptual approach to accurately simulate photon recycling is illustrated in Fig. 2. The optical absorption associated with a given photovoltaic structure is fed into a drift–diffusion model, which produces a charge carrier distribution. This charge carrier distribution can then be used to create a radiative recombination profile that feeds back into the optical absorption data. When the iterative feedback loop converges to a stable charge carrier profile, the result
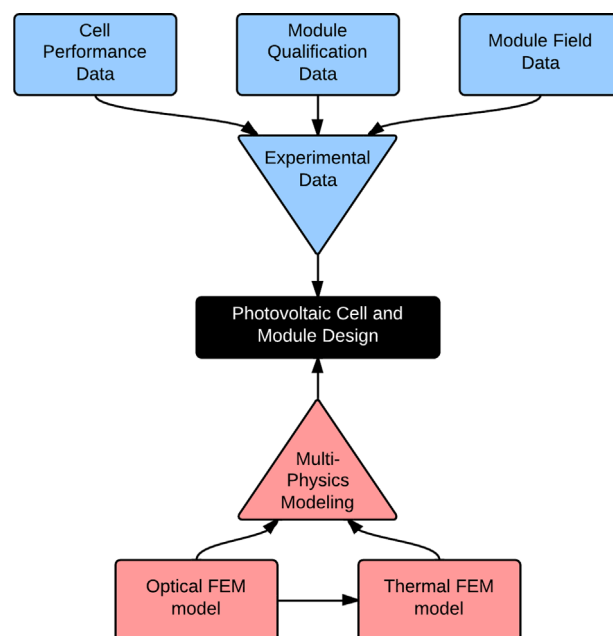
is taken to be accurate and self-consistent. Of course, ultimate verification must come from careful comparison to experiment.

Based on the simulation procedure alone, it can be seen that the magnitude of the correction is closely related to the external radiative efficiency of a PV cell, defined as the probability that a recombination event inside the cell results in an externally emitted photon. Thus, the correction observed with cells having very low external radiative efficiencies, such as amorphous silicon thin-film PV cells, will be extremely modest [3,36]. On the other hand, predictions for cells exhibiting high external radiative efficiencies, such as epitaxial thin films of III–V materials, will be significantly different when using this approach compared to conventional optical and electronic models [38]. This approach of modeling photon recycling by combining drift–diffusion and full-wave optical models in a self-consistent fashion has been shown to be necessary to achieve predictions closely matching the observed performances of cells by Alta Devices [38–40].

5. Reliability

The final example of combining full-wave optical modeling with additional physics to probe important physics is the problem of intrinsic reliability. Recent work from Roger French at Case Western has identified the dominant pathways to intrinsic failures in PV encapsulant materials: EVA yellowing and PET hydrolysis [66]. Ethylene vinyl acetate (EVA, also known as STR Photocap or DuPont Elvax) was identified in the early stages of PV manufacturing as an ideal encapsulant thanks to low costs and high reliability. However, certain issues remain, particularly EVA yellowing, which degrades optical absorption and causes further heating. This is believed to be caused by formation of chromophores in the presence of heat and ultraviolet light over extended time periods. The precise mechanisms and rates of degradation have been carefully characterized for multiple grades of EVA, through careful comparison of Xe arc lamp and field measurement data [67]. This process can also be partially
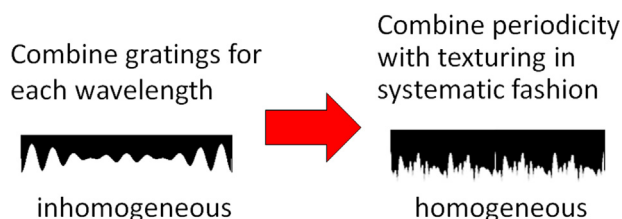
Fig. 3. Illustration of the interaction between multiphysics numerical modeling and experimental data used in designing photovoltaic cells and modules for high reliability. Multiphysics models are used to predict possible failure modes due to localized absorption hot spots that cause thermal overload. These predictions are then compared to performance data at the cell level, plus qualification and field data at the module level. This process can be iterated multiple times to help improve reliability.

reversed, particularly around the edges with oxidative bleaching. However, further study is still required for more complex interactions that may occur in field-installed systems, particularly ion and silver migration. Polyethylene terephthalate (PET) is generally employed as an inexpensive moisture barrier. However, its extended exposure to moisture creates the potential for hydrolysis, which in turn is considered to pose multiple risks. In particular, hydrolysis can foster the creation of micropores, which allow for moisture ingress. This can also affect the interior EVA layer by promoting hydrolysis and delamination, which can then, in turn, both directly reduce module performance and also corrode the metallic wiring.

Both the thermal and optical performance over time of an idealized photovoltaic module constructed from these materials and subjected to these real-world effects can be captured using a single parametric multiphysics model. In this approach, both the initially specified and degraded structures are specified in terms of their geometric and physical parameters. This family of structures can then be discretized on an automatically generated tetrahedral basis.

This FEM simulation can then be used to find the distribution of light and heat through a thin-film PV multilayer stack with certain non-trivial features, including textured glass with transparent conductive oxides, anti-reflection coatings, front contact grids, back-surface layers, emitter wrap-through, and laser scribing. This data will then allow the direct detection of localized regions of heating and UV exposure caused by, e.g., yellowing of materials in the light path, Ohmic light absorption at the metal, series resistance, and shunting. This will give rise to projected maximum-power point performance, as well as a 3D temperature distribution in the various device layers, as well as the adjoining module structures, including encapsulants.

Using microscopic degradation rates of the relevant materials, the level of heating projected can be linked to a rate of change in the overall structures, which can then be fed back into the model in Section 2 to predict failure statistics (including mean time between failures, rate of early failure, maximum lifetime, etc.). The microscopic rates are derived from a physics-based approach, which employs a combination of multiple experimental data directly from operating PV field data as well as accelerated lifetime testing, along with cross-checked single-molecule experiments and *ab initio* quantum chemistry predictions. Distinct degradation rates can then be obtained from first principles for each of the key components with potential intrinsic reliability concerns.

Fig. 3 demonstrates an overall approach to combining the disparate types of numerical modeling and experimental data to achieve high reliability photovoltaic modules. Multiphysics models are used to predict possible failure modes due to localized absorption hot spots that cause thermal overload. These predictions are then compared to performance data at the cell level, plus qualification and field data at the module level. This process can be iterated as many times as needed in order to improve reliability.

6. Conclusions

In conclusion, three case studies were considered in which the tools of full-wave optical modeling, such as MEEP [41], can be combined with other physics-based models to address three significant problems in photovoltaics: enhancing light trapping with subrandom noise structures, recycling re-radiated photons, and reducing intrinsic failures. While the preliminary results in all cases look promising, these problems still deserve a great deal of further study before they can be considered to be solved, both from a modeling and experimental perspective. In particular, applying these approaches to 3D problems with complex geometries has not yet been fully studied, but deserves further investigation in the near term, as they could significantly impact the goal of improved photovoltaic cells in the long term.

References

[1] M.A. Green, Solar Cells: Operating Principles, Technology, and System Applications, University of New South Wales Press, Sydney, Australia, 1992.
[2] R.F. Pierret, Semiconductor Device Fundamentals, Addison-Wesley, Reading, MA, 1996.
[3] M.A. Green, K. Emery, Y. Hishikawa, W. Warta, E.D. Dunlop, Prog. Photovolt. 21 (2013) 827.
[4] M.A. Green, Prog. Photovolt. 9 (2001) 123.
[5] K.L. Chopra, P.D. Paulson, V. Dutta, Prog. Photovolt.: Res. Appl. 12 (2004) 69.
[6] M.S. Keshner, R. Arya, Study of potential cost reductions resulting from super-large-scale manufacturing of PV modules, SR-520-36846, NREL, Golden, CO, 2004.
[7] M.A. Green, J. Mater. Sci. 18 (2007) 15.
[8] B. von Roedern, H.S. Ullal, in: Proceedings of the IEEE Photovoltaics Specialists Conference, vol. 33, 2008, pp. 1–4.
[9] C. Wadia, A.P. Alivisatos, D.M. Kammen, Environ. Sci. Technol. 43 (2009) 2072.
[10] S.E. Habas, H.A.S. Platt, M.F.A.M. van Hest, D.S. Ginley, Chem. Rev. 110 (2010) 6571.
[11] L. Stolt, J. Hedstrom, J. Kessler, M. Ruckh, K.O. Velthaus, H.W. Schock, Appl. Phys. Lett. 62 (1993) 597.
[12] K. Siemer, J. Klaer, I. Luck, J. Bruns, R. Klenk, D. Braunig, Sol. Energy Mater. Sol. Cells 67 (2001) 159.
[13] I. Repins, M.A. Contreras, B. Egaas, C. DeHart, J. Scharf, C.L. Perkins, B. To, R. Noufi, Prog. Photovolt. 16 (2008) 235.
[14] P. Jackson, D. Hariskos, E. Lotter, S. Paetel, R. Wuerz, R. Menner, W. Wischmann, M. Powalla, Prog. Photovolt.: Res. Appl. 19 (2011) 894.
[15] EMPA Press Release, January 18, 2013, available at: ⟨http://www.empa.ch/plugin/template/empa/3/131438/−/l=2⟩ (accessed 28.09.13).
[16] First Solar Press Releases, February 26 and April 9, 2013. available at: ⟨http://investor.firstsolar.com/releasedetail.cfm?releaseid=743398⟩ and ⟨http://investor.firstsolar.com/releasedetail.cfm?releaseid=755244⟩ (accessed 28.09.13).
[17] M. Despeisse, C. Ballif, A. Feltrin, F. Meillaud, S. Fay, F.J. Haug, D. Domine, M. Python, T. Soderstrom, P. Buehlmann, G. Bugnon, Proc. SPIE 7409 (2009) 74090B.
[18] S.W. Ahn, S.E. Lee, H.M. Lee, in: Proceedings of the European Photovoltaic Solar Energy Conference, vol. 27, 2012, 3AO5.1.
[19] B. Ray, P.R. Nair, R.E. García, M.A. Alam, in: Proceedings of the International Electron Devices Meeting, 2009.
[20] B. Ray, P.R. Nair, M.A. Alam, in: Proceedings of the IEEE Photovoltaics Specialists Conference, vol 35, 2010, pp. 85–89.
[21] B. Ray, P. Nair, M.A. Alam, Sol. Energy Mater. Sol. Cells 95 (2011) 3287.
[22] B. Ray, P. Nair, M.A. Alam, Appl. Phys. Lett. 99 (2011) 033003.
[23] R. Service, Science 332 (2011) 293.
[24] J. Allen, K. Yager, H. Hlaing, C. Nam, B. Ocko, C. Black, Appl. Phys. Lett. 99 (2011) 163301.
[25] A. Mihi, H. Miguez, J. Phys. Chem. B 109 (2005) 15968.
[26] C. Huisman, J. Schoonman, A. Goossens, Sol. Energy Mater. Sol. Cells 85 (2005) 115.

[27] R. Komiya, A. Fukui, N. Murofushi, N. Koide, R. Yamanaka, H. Katayama, in: Proceedings of the International Photovoltaic Science and Engineering Conference, vol. 21, 2011, 2C-5O-08.

[28] W. Shockley, H.J. Queisser, J. Appl. Phys. 32 (1961) 510.

[29] C.H. Henry, J. Appl. Phys. 51 (1980) 4494.

[30] W. van Roosbroeck, W. Shockley, Phys. Rev. 94 (1954) 1558.

[31] S.S. Hegedus, A. Luque, Handbook of Photovoltaic Science and Engineering, Wiley, Chichester, 2003.

[32] R.F. McCarthy, H.W. Hillhouse, in: Proceedings of the IEEE Photovoltaics Specialists Conference, vol. 38, 2012, pp. 1663–1668.

[33] R.J. Schwartz, M.S. Lundstrom, in: Proceedings of the Solar Cell High Efficiency and Radiation Damage Meeting, vol. 4, 1980.

[34] M.S. Lundstrom, J.L. Gray, R.J. Schwartz, Proceedings of the NASECODE Conference, vol. 2, 1981, pp. 223–227.

[35] M.S. Lundstrom, R.J. Schwartz, J.L. Gray, in: Proceedings of the IEEE Photovoltaics Specialists Conference, vol. 15, 1981, pp. 400–405.

[36] M.R. Khan, P. Bermel, M.A. Alam, in: Proceedings of the IEEE Photovoltaics Specialists Conference 39, 2013, 1.

[37] J.L. Gray, X. Wang, X. Sun, ADEPT 2, Available at: ⟨http://nanohub.org/resources/adeptnpt⟩ (accessed 28.09.13).

[38] X. Wang, M.R. Khan, J.L. Gray, M.A. Alam, M.S. Lundstrom, IEEE J. Photovolt. PP99 (2013) 1.

[39] X. Wang, M.R. Khan, M.A. Alam, M. Lundstrom, in: Proceedings of the IEEE Photovoltaics Specialists Conference, vol. 38, 2012, pp. 2117–2121.

[40] X. Wang, M.S. Lundstrom, IEEE J. Photovolt. 3 (2013) 1348.

[41] A.F. Oskooi, D. Roundy, M. Ibanescu, P. Bermel, J.D. Joannopoulos, S.G. Johnson, Comput. Phys. Commun. 181 (2010) 687.

[42] FAESOR Package, September 13, 2012, available at: ⟨http://hogwarts.ucsd.edu/~pkrysl/faesor/faesor_publish.html⟩ (accessed 28.09.13).

[43] P. Krysl, Thermal and Stress Analysis with the Finite Element Method, Pressure Cooker Press, San Diego, CA, 2010.

[44] COMSOL Multiphysics version 4.3a, available at: ⟨http://www.comsol.com/⟩ (accessed 28.09.13).

[45] E. Yablonovitch, G. Cody, IEEE Trans. Electron Devices 29 (1982) 300.

[46] T. Tiedje, E. Yablonovitch, G. Cody, B. Brooks, IEEE Trans. Electron Devices 31 (1984) 711.

[47] P. Campbell, M.A. Green, J. Appl. Phys. 62 (1987) 243.

[48] R. Brendel, Thin-Film Crystalline Silicon Solar Cells, Wiley-VCH, Weinheim, Germany, 2003.

[49] P. Bermel, C. Luo, L. Zeng, L.C. Kimerling, J.D. Joannopoulos, Opt. Express 15 (2007) 16986.

[50] Z. Yu, A. Raman, S. Fan, Proc. Natl. Acad. Sci. USA 107 (2010) 17491.

[51] R. Brendel, M. Hirsch, R. Plieninger, J. Werner, IEEE Trans. Electron Devices 43 (1996) 1104.

[52] J. Gee, in: Proceedings of the IEEE Photovoltaics Specialists Conference 29, 2002, 150.

[53] K. Wada, L.C. Kimerling, N. Toyoda, Back Reflector of Solar Cells, US Patent 6750393, 2004.

[54] L. Zeng, Y. Yi, C.-Y. Hong, X. Duan, L.C. Kimerling, Mater. Res. Soc. Symp. Proc. 862 (2005) 1.

[55] L. Zeng, P. Bermel, Y. Yi, N. Feng, C.-Y. Hong, X. Duan, J.D. Joannopoulos, L.C. Kimerling, Mater. Res. Soc. Symp. Proc. 974E (2006) 1.

[56] D.-H. Ko, J.R. Tumbleston, A. Gadisa, M. Aryala, Y. Liu, R. Lopez, E.T. Samulski, J. Mater. Chem. 21 (2011) 16293.

[57] Y.-C. Liu, C. Kirsh, A. Gadisa, M. Aryal, S. Mitran, E.T. Samulski, R. Lopez, J. Phys. D 46 (2013) 024008.

[58] J.B. Kim, P. Kim, N.C. Pegard, S.J. Oh, C.R. Kagan, J.W. Fleischer, H.A. Stone, Y.-L. Loo, Nat. Photon. 6 (2012) 327.

[59] H. Katagiri, K. Jimbo, W.S. Maw, K. Oishi, M. Yamazaki, H. Araki, A. Takeuchi, Thin Solid Films 517 (2009) 2455.

[60] J. Paier, R. Asahi, A. Nagoya, G. Kresse, Phys. Rev. B 79 (2009) 115126.

[61] Q. Guo, H. Hillhouse, R. Agrawal, J. Am. Chem. Soc. 131 (2009) 11672.

[62] G.M. Ford, Q. Guo, R. Agrawal, H. Hillhouse, Chem. Mater. 23 (2011) 2626.

[63] X. Sheng, S.G. Johnson, J. Michel, L.C. Kimerling, Opt. Express 19 (2011) A841.

[64] Y.-L. Lu, L. Li, K.A. Reinhardt, Mater. Sci. Forum 636 (2010) 855.

[65] I. Schnitzer, E. Yablonovitch, C. Caneau, T.J. Gmitter, Appl. Phys. Lett. 62 (1993) 131.

[66] R.H. French, M.P. Murray, W.-C. Lin, K.A. Shell, S.A. Brown, M.A. Schuetz, R.J. Davis, IEEE Energytech 2011 (2011) 1.

[67] S.A. Gevorgyan, A.J. Medford, E. Bundgaard, S.B. Sapkota, H.-F. Schleiermacher, B. Zimmermann, U. Würfel, A. Chafiq, M. Lira-Cantu, T. Swonke, M. Wagner, C.J. Brabec, O. Haillant, E. Voroshazi, T. Aernouts, R. Steim, J.A. Hauch, A. Elschner, M. Pannone, M. Xiao, A. Langzettel, D. Laird, M.T. Lloyd, T. Rath, E. Maier, G. Trimmel, M. Hermenau, T. Menke, K. Leo, R. Rösch, M. Seeland, H. Hoppe, T.J. Nagle, K.B. Burke, C.J. Fell, D. Vak, T.B. Singh, S.E. Watkins, Y. Galagan, A. Manor, E.A. Katz, T. Kim, K. Kim, P.M. Sommeling, W.J.H. Verhees, S.C. Veenstra, M. Riede, M.G. Christoforo, T. Currier, V. Shrotriya, G. Schwartz, F.C. Krebs, Sol. Energy Mater. Sol. Cells 95 (2011) 1398.